ELSEVIER

Thermochimica Acta 256 (1995) 309–324

thermochimica acta

Combustion of some zinc-fuelled binary pyrotechnic systems

Michael J. Tribelhorn, Dean S. Venables, Michael E. Brown *

Chemistry Department, Rhodes University, Grahamstown 6140, South Africa

Received 18 August 1994; accepted 22 December 1994

Abstract

Combustion studies of several binary pyrotechnic systems using zinc as fuel and one of the oxidants: PbO_2, Pb_3O_4, PbO, BaO_2, SrO_2 or $KMnO_4$, are reported. Combustion was very sensitive to compaction, and only mixtures of Zn/PbO_2, Zn/Pb_3O_4 and $Zn/KMnO_4$ sustained combustion when compacted. In all of the systems studied, the temperatures measured during passage of the combustion front past an imbedded thermocouple rapidly rose above the melting point of zinc. Burning rates were recorded for the Zn/PbO_2 system compacted under 50 MPa, and the $Zn/KMnO_4$ system under 50, 100 and 150 MPa. Thermochemical and kinetic data were determined where possible. Combustion mechanisms are suggested, involving condensed phase, diffusion-controlled reactions and gas-phase reactions occurring in parallel. Analysis of residues shows that ZnO is the major product in the Zn/PbO_2 and Zn/Pb_3O_4 systems, and that mixed zinc oxides are possibly the major products of the $Zn/KMnO_4$, Zn/BaO_2 and Zn/SrO_2 systems.

Keywords: Binary system; Compaction; Combustion; Mechanism; Mixed oxide; Pyrotechnic; Zinc

1. Introduction

Very little work has been published on the use of Zn as a fuel in pyrotechnic delays, although the use of Zn in smoke-producing compositions has been investi-

* Corresponding author.

SSDI 0040-6031(95)02248-1

gated. The present study complements a detailed thermoanalytical study [1] of the individual reactants and the binary systems.

During combustion of Zn/oxidant pyrotechnic systems, the temperature rises rapidly to well above the melting point of Zn (419.5°C) and even above its standard boiling point at 908°C. Derevyaga et al. [2] reported that the combustion of Zn takes place both at the liquid surface and in the surrounding gas space. The kinetics of the oxidation of molten Zn have been examined in detail by Cope [3], who confirmed that the rate of growth of ZnO on molten Zn followed the parabolic law. He proposed that the oxidation of Zn is controlled by the diffusion of defects, associated with the excess-metal character of non-stoichiometric zinc oxide, through the oxide layer.

Most of the oxidants used in this study (PbO_2, Pb_3O_4, BaO_2, SrO_2 or $KMnO_4$) decompose without melting to produce oxygen gas and a solid residue [1]. The reactions of the pyrotechnic mixtures may thus be solid–solid, liquid–solid, liquid–gas, solid–gas, or even gas–gas reactions.

Lead oxides have been used as oxidants in several pyrotechnic systems, particularly with silicon or boron as the fuels [4,5]. The Ta/PbO_2 and Ta/Pb_3O_4 systems have also been investigated [6]. Reactions of fuel/PbO_2 systems are usually more rapid than in the fuel/Pb_3O_4 systems under similar conditions. This difference is ascribed to the production of more active Pb_3O_4 from freshly decomposed PbO_2.

The use of barium peroxide and strontium peroxide in pyrotechnic systems is common [7], e.g. strontium peroxide has been used in flares in conjunction with other oxidising agents to obtain a red flame, whilst barium peroxide finds use chiefly in delay compositions.

Spice and Staveley [8,9] studied the Fe/BaO_2, S/BaO_2, Mo/BaO_2 and Mn/BaO_2 systems. Hill et al. [10] published data on the Mo/BaO_2, Fe/BaO_2 and S/BaO_2 systems. Booth [11] used the Fe/BaO_2 system to test his mathematical theory of self-propagating layer-to-layer combustion. Hogan and Gordon [12] studied the Mg/BaO_2 and the Mg/BaO_2/calcium resinate systems. Nakahara [13] and Hikita [14,15] studied the temperature and pressure characteristics of a variety of systems including the Fe/BaO_2 and Mo/BaO_2 systems. They concluded that the combustion wave in the iron system is preceded by flowing gas arising from the endothermic decomposition of the oxidant.

Johnson [16] investigated the Se/BaO_2 delay system for the effect of pre-heating and found that the pre-ignition reaction was not self-sustaining. His findings that the Se diffuses in the lattice to form a surface coating of product prior to ignition, followed by bulk reactions, are in agreement with the conclusions reached by Hill and Wallace [17,18] in their study on the Mo/$KMnO_4$ system, and Spice and Staveley's research on Fe/BaO_2 and Fe/$K_2Cr_2O_7$ [8,9].

Beyens and Dubois [19] studied the Mg/BaO_2 system and reported that the particle shape played a significant role in the thermal behaviour of BaO_2. They also studied the effect of the formation of surface $BaCO_3$ on burning, and noted a decrease in burning rate on exposure in humid air.

Potassium permanganate has also been extensively used as an oxidant in pyrotechnic delay compositions. Hill and Wallace [17], in a study of the Mo/$KMnO_4$

system, observed two stages in the reaction. The first (occurring below 120°C) was proposed to involve the most mobile species, Mo, coating the internal surfaces with a layer of product by migrating along the grain boundaries. The activation energy of this process is low, and hence reaction occurs relatively rapidly at low temperatures. This stage is followed by the second reaction in which penetration of the mosaic is energetically possible, and reaction with the bulk can occur (at 850°C). The activation energy of this process is higher (between 20 and 40 kJ mol^{-1} for Fe, Sb, and Mo systems), and hence the process is slow at low temperatures. The $Fe/KMnO_4$, $Fe/K_2Cr_2O_7$ and Fe/BaO_2 system [18] were reported to react in an analogous manner.

Beck and Brown [20,21] have made a detailed study of the commercially important $Sb/KMnO_4$ system. Combustion involves gaseous intermediates, including $O_2(g)$ from decomposition of the oxidant, and possibly $Sb_2O_3(g)$. Burning rates were very dependent upon composition, fuel particle-size, container material and venting, and the presence of additives. Some results for the $Se/KMnO_4$ system were also reported [21].

2. Experimental

2.1. Materials

The materials used [1] were zinc powder (<5 μm, 94% pure), lead dioxide (<75 μm), and red lead (<75 μm), which were supplied by AECI Ltd. The yellow lead monoxide (massicot) (<250 μm) was supplied by BDH Ltd. Barium peroxide (85% pure, <20 μm) was obtained from Saarchem, and strontium peroxide (88% pure, <20 μm) from Bernardy Chemie, France. $KMnO_4$ powder (<53 μm) was supplied by AECI Ltd. Mixtures were prepared by tumbling in the presence of rubber balls for 1 h. The compositions of fuel/oxidant mixtures are described in terms of the mass percentage of fuel.

The particle-size distribution of the zinc powder was determined by scanning electron microscopy (SEM), which showed that the zinc consisted largely of small spheres of less than 4 μm diameter, together with a few large agglomerates which were about 10 μm in diameter. The mean diameter of the particles was approximately 1.0 μm.

2.2. Apparatus

The equipment used for the measurement of burning rates and temperature profiles has been described [7].

Scanning electron microscopy (SEM) (Joel JSM-840) was used to examine the shapes and surface appearance of the individual reactant powders and the reaction residues, and X-ray diffraction (XRD) and infrared spectroscopy were used to try to identify the reaction products.

2.3. Data processing

Temperature profiles were processed in a number of steps. A simple filter program was used to remove deviations caused by noise, and the data were then averaged to reduce the number of points for subsequent processing. Finally, the profiles were smoothed using a 15-point cubic least-squares Savitsky–Golay convolution procedure [22]. Kinetic parameters were derived following the Leeds approach [23,24], which included use of a non-linear optimisation routine in the BMDP statistical software package [25].

3. Results and discussion

3.1. Burning rates, temperature profiles and combustion products

3.1.1. Zinc/lead oxide systems

Zn burned in combination with each of PbO_2, Pb_2O_4, and PbO over a wide range of compositions (10–70% Zn). The stoichiometric mass ratios were difficult to estimate on account of the complex behaviour of the lead oxides [1]. When compacted under 55 MPa, however, only Zn/PbO_2 sustained combustion (over the range 20–45% Zn; the stoichiometric proportion of Zn is 21.5% based on $PbO_2 \rightarrow PbO$, or 35.4% by mass for $PbO_2 \rightarrow Pb$). Burning rates increased with increasing proportion of fuel as shown in Table 1. At higher compactions (110 MPa) this system burned from 25% to 45% Zn. When compacted by hand, the Zn/Pb_3O_4 system was able to sustain combustion for compositions of 25–40% Zn. Mixtures of Zn/PbO were not able to sustain combustion even under minimal compaction. Reliable burning rates for Zn/Pb_3O_4 and Zn/PbO (compacted by hand) could not be obtained. Some initial studies of $Zn/PbO_2/PbO$ mixtures showed that this ternary system burned reasonably steadily under 50 MPa pressure. Less gas was evolved than in the equivalent PbO_2 system, and the burning rates were somewhat slower.

All of the systems evolved a fair amount of gas during combustion, which often caused expulsion of solids from the channel. Higher percentage Zn compositions were more gassy than other compositions, and burned a lot more rapidly and violently. The gas evolved may be O_2 from decomposition of the oxidant, but could

Table 1
Burning rates v of Zn/PbO_2 compositions (55 MPa compaction)

Zn/%	v/(mm s^{-1})	Zn/%	v/(mm s^{-1})
20	2.21 ± 0.15	35	13.7 ± 2.2
25	4.36 ± 1.07	45	$27.2 \pm ?$
30	11.1 ± 2.1	50	$90.2 \pm ?$
40	12.6 ± 6.4		

also include Zn or even Pb vapour, owing to the high temperatures achieved during reaction. Since higher proportions of zinc result in more gassy reactions, Zn vapour is the most likely intermediate.

Products from combustion of low-percentage Zn compositions (20–35% Zn) showed an appreciable yellow colour, probably from PbO. Residues of combustion of compositions with excess Zn were grey in colour, and a deposit of silver-grey metal was observed at the bottom of the channel.

IR spectra of the residues of Zn/PbO_2 and Zn/Pb_3O_4 combustion showed only very weak absorptions. None corresponded to the peaks expected in the ZnO spectrum (at 1300, 1350, 730, and from 350 to 600 cm^{-1}) [26].

XRD of the residues of Zn/PbO_2 combustion showed the presence of considerable PbO, formed by decomposition or partial reduction of PbO_2, along with ZnO and Pb in small quantities. The quantity of ZnO and Pb increased with increasing percentage of zinc in the compositions and unreacted Zn was also detected. XRD of the residues of Zn/Pb_3O_4 combustion showed minimal PbO, but considerable Pb, indicating that the oxidant had been fully reduced. ZnO was also present.

Temperature profiles were recorded for various compositions of the Zn/PbO_2 and Zn/Pb_3O_4 systems. Profiles were not very reproducible in shape or maximum temperature values. Using thermocouples of larger diameter and changing the compaction of the mixture did not significantly improve the reproducibility of the temperature profiles. The maximum temperatures reached during the combustion of all the Zn/PbO_2 mixtures and many of the Zn/Pb_3O_4 mixtures were well over the 1800°C maximum operating temperature of the S-type thermocouples. Maximum temperatures in some Zn/Pb_3O_4 compositions were lower (1000–1400°C). There is also the possibility of Zn and Pb reacting with the Pt thermocouples. Temperature profiles of these systems were not suitable for kinetic analysis, particularly because the theory on which kinetic analysis is based [23] is strictly only applicable to gasless combustion.

3.1.2. Zinc/peroxide systems

Zn/BaO_2. Zn/BaO_2 compositions supported combustion over a wide range (10–65% zinc) in the uncompacted state, but attempts to initiate combustion of material compacted at 55 MPa failed. Temperature profiles of uncompacted powder showed a rapid rise to maximum temperature, but mixtures which had been compacted showed a relatively gradual rise. Thermal analysis [1] confirmed that the zinc melts prior to reaction. The gaseous nature of the reaction is also apparent from the flame generated by the mixture. Addition of 10% ZnO to the system resulted in less vigorous burning of uncompacted powder. Burning rates for uncompacted and very lightly compacted (200 kPa) compositions are given in Table 2.

Temperature profiles of uncompacted mixtures were recorded, but thicker (0.2 mm) thermocouples were necessary to remove the effects of noise generated by physical movement of the thermocouple junction, i.e. to reduce the sensitivity of the response. Reproducibility was still poor as is shown in Fig. 1.

IR spectra of the products of combustion of the Zn/BaO_2 system showed that the absorption bands at 3570, 1750, 1430 and 850 cm^{-1} occurring in the BaO_2

Table 2
The variation of burning rate v with composition and compaction of the Zn/BaO_2 system

Zn/%	v/(mm s^{-1}) for 0 Pa	v/(mm s^{-1}) for 200 Pa
10	4.2 ± 0.1	–
15	5.1 ± 0.2	–
20	9.7 ± 0.6	
25	14.6 ± 1.4	–
30	21.0 ± 2.9	7.5 ± 0.4
35	37.6 ± 9.4	10.5 ± 0.7
40	48.4 ± 22.7	15.2 ± 1.5
45	75.2 ± 37.7	32.9 ± 7.2
50	42.3 ± 11.9	29.7 ± 5.9
55	29.8 ± 5.9	17.5 ± 2.0
60	12.5 ± 1.0	–
65	4.9 ± 0.2	–

spectrum were decreased in intensity or removed, while a new peak appeared at 730 cm^{-1} due to the formation of ZnO.

Zn/SrO_2. Zn/SrO_2 compositions behaved similarly to the Zn/BaO_2 compositions, with the uncompacted mixtures burning in the range 25–80% Zn. Very light compaction (200 kPa) decreased the burning range to 30–55% Zn. Burning rates are given in Table 3. The reactions were less vigorous than those of BaO_2, and T_{max} and the burning rates were decreased. Temperature profiles were not very reproducible as shown in Fig. 2.

The IR spectra of the residue from combustion of the Zn/SrO_2 system differed from that of the starting material by the loss of the Sr–O stretch at 3490 cm^{-1} and decreased intensities of the peaks at 1450, 1020 and 850 cm^{-1}. No trace of the ZnO absorption was apparent at 730 cm^{-1}.

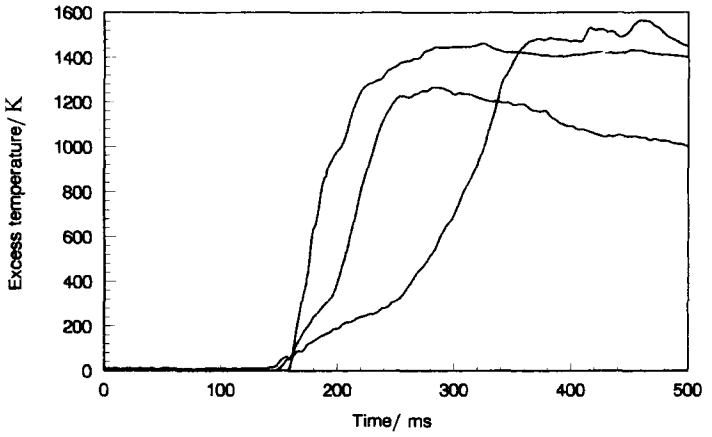

Fig. 1. Replicate temperature profiles for combustion of uncompacted 30% Zn/BaO_2 compositions.

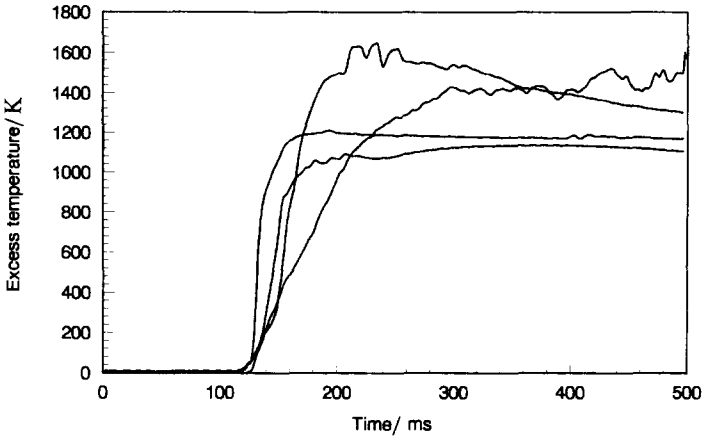

Fig. 2. Replicate temperature profiles for combustion of uncompacted 30% Zn/SrO_2 compositions.

XRD of the residues of combustion of the zinc/peroxide systems suggests the formation of mixed oxides, with $SrZnO_2$ and ZnO (including some unreacted Zn) peaks appearing in the 50% Zn/SrO_2 residue (yet no SrO), and $BaZnO_2 \cdot 2H_2O$ and ZnO (again with unreacted Zn, but no BaO) peaks appearing in the residue of the 50% Zn/BaO_2 system. At lower Zn levels, ZnO and BaO (or SrO) were present.

3.1.3. The zinc/potassium permanganate system

$Zn/KMnO_4$ compositions burned over the range 30–75% Zn when compacted under 55 MPa. Linear burning rates are given in Table 4. Compositions low in Zn burned slowly and reproducibly, and did not evolve much gas. The burning rates increased approximately linearly with increasing Zn content (30–50% Zn). At 55% Zn, the burning rate increased sharply and much gas was evolved. Similar rapid, gaseous reaction was observed for compositions richer in fuel, although a slight

Table 3
The variation of burning rate v with composition and compaction of the Zn/SrO_2 system

Zn/%	v/(mm s^{-1}) for 0 Pa	v/(mm s^{-1}) for 200 kPa
30	5.1 ± 0.2	4.3 ± 0.1
35	10.2 ± 0.7	5.5 ± 0.2
40	15.7 ± 1.6	7.6 ± 0.4
45	20.8 ± 2.9	12.3 ± 1.0
50	24.9 ± 4.1	10.1 ± 0.7
55	22.3 ± 3.3	6.2 ± 0.3
60	19.8 ± 2.6	–
65	15.4 ± 1.6	–
70	9.8 ± 0.6	–
75	6.7 ± 0.3	–
80	4.8 ± 0.2	–

Table 4
Variation of burning rates v with composition and compaction of the $Zn/KMnO_4$ system

Zn/%	v/(mm s^{-1})		
	55 MPa	110 MPa	165 MPa
35	2.1 ± 0.1	2.1 ± 0.1	1.9 ± 0.1
45	7.3 ± 0.3	6.2 ± 0.1	6.0 ± 0.2
50	10.4 ± 0.8	8.8 ± 1.1	8.7 ± 1.0
55	74 ± 50	16.4 ± 0.9	12.4 ± 2.7
60	70 ± 58	23.1 ± 2.3	21.3 ± 0.9
65	46 ± 14	24.0 ± 8.1	23.2 ± 4.9
70	39 ± 10	21.9 ± 1.3	15.0 ± 1.2

decrease in burning rate was observed at the upper end of the burning range. The fastest average burning rate occurred in compositions containing 55–60% Zn, and was about 75 mm s^{-1}. There were considerable variations in individual burning rates recorded at these compositions. Increasing the pressure of compaction to 110 MPa caused a decrease in the burning rates of the mixtures. This decrease was pronounced in the more gaseous reactions, i.e. compositions of 55% Zn and over, and there was a large drop in the maximum burning rate. Further decreases in burning rate occurred when mixtures were compacted under 150 MPa, especially in fuel-rich mixtures. Burning rates are reported in Table 4.

The limited reproducibility of the temperature profiles for a 35% $Zn/KMnO_4$ composition, recorded with 0.1 mm-diameter with thermocouples, is illustrated in

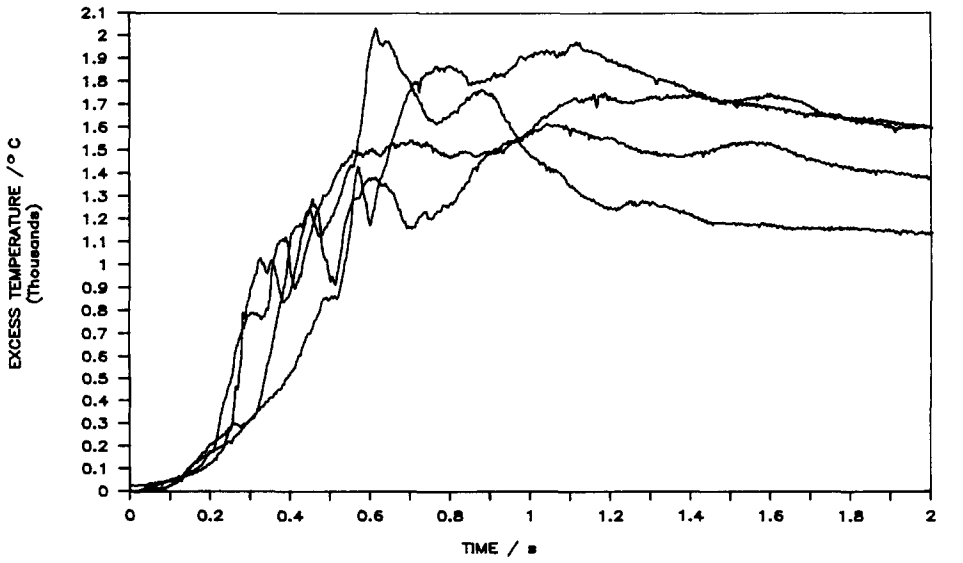

Fig. 3. Replicate temperature profiles for combustion of 35% $Zn/KMnO_4$ composition, compacted at 50 MPa.

Table 5
Kinetic parameters obtained by application of the Leeds approach to the Zn/oxidant systems

Zn/%	E_a/(kJ mol^{-1})	A/s^{-1}	n
Zn/BaO_2 system			
30	16.0 ± 3.5	241 ± 54	0.64 ± 0.06
35	13.8 ± 1.6	224 ± 59	0.54 ± 0.06
40	19.0 ± 4.9	522 ± 186	0.63 ± 0.01
45	6.9 ± 1.8	170 ± 10	0.64 ± 0.06
50	6.7 ± 1.1	146 ± 32	0.51 ± 0.03
Zn/SrO_2 system			
30	10.8 ± 0.8	96 ± 13	0.54 ± 0.02
35	9.5 ± 1.5	70 ± 22	0.60 ± 0.08
40	10.2 ± 0.9	94 ± 7	0.71 ± 0.06
45	10.4 ± 1.0	146 ± 30	0.54 ± 0.05
50	16.0 ± 3.3	181 ± 51	0.64 ± 0.07
35% Zn/$KMnO_4$			
	17.1	7.12 ± 10^4	0.54
	10.0	2.20 ± 10^4	0.39
	34.0	1.50 ± 10^6	0.37

Fig. 3. Several features are common to the profiles. These include a small step at low temperatures (250–350°C), as well as one, or sometimes two, sudden decreases in temperature over a short time interval. These decreases in temperature usually occurred between 800 and 1000°C, and between 1100 and 1400°C, and possibly result from the vaporisation of a species in the mixture, or the formation of gas pockets over the thermocouple. These irregularities in the profiles indicate that a number of different thermal events occur at different stages in the combustion.

Temperature profiles of different compositions showed an increase in maximum temperature with increasing fuel content, but profiles were less reproducible owing to increased gas evolution. Increasing the thermocouple wire diameter gave smoother profiles, as did increasing the compaction pressure of the mixtures. Assuming a linear relationship between thermocouple wire diameter and maximum temperature, extrapolation to zero thickness gives a maximum temperature of 1820 ± 120°C for the 35% Zn/$KMnO_4$ composition under 55 MPa compaction.

Residues from combustion of mixtures containing 30–50% Zn were dark green and very hygroscopic. In the faster, gassy reactions, the centre of the residue had been hollowed out by the evolved gases. Residues from the most fuel-rich mixtures (65–75% Zn) were red-brown, brittle and crusty.

IR spectra of the residues of combustion of Zn/$KMnO_4$ compositions suggested the presence of K_2MnO_4 and/or K_3MnO_4 in the residue. K_2MnO_4 and K_3MnO_4 are products of the decomposition of $KMnO_4$. The reaction of Zn with K_2MnO_4 and K_3MnO_4 to form mixed Zn oxides may account for the absence of these decomposition products in higher fuel compositions. No absorptions characteristic of ZnO were observed. Quantitative measurements of the amounts of K_2MnO_4 in the residue showed a decrease from 10% in the 30% Zn/$KMnO_4$ residue to 0% in

the 50% $Zn/KMnO_4$ residue. These observations suggest that two types of reaction operate in the $Zn/KMnO_4$ system. In compositions low in fuel, where the mixtures burn slowly and steadily and do not produce much gas, the reaction between liquid Zn and solid oxidant (the products of the first stage of the decomposition of $KMnO_4$) is probably diffusion-controlled. In fuel-rich mixtures, the reaction becomes very much faster and more gaseous, indicating the participation of Zn vapour. At higher packing pressures (110 and 165 MPa), the burning rate decreased very slightly in compositions low in Zn (as expected for diffusion-type reactions), but mixtures rich in fuel exhibited large decreases in burning rate on compaction, as expected for reactions involving a gaseous participant.

3.2. Kinetics

Attempts were made to extract approximate kinetic parameters for the combustion reactions of the Zn/peroxide and Zn/permanganate systems using the Leeds approach [23,24]. Kinetic data extracted from the best profiles are shown in Table 5. The apparent activation energies obtained are all low (between 7 and 35 kJ mol^{-1}) in keeping with the diffusion-type mechanisms proposed [24] to govern combustion of most pyrotechnic systems.

3.3. Thermochemistry

Thermodynamic data [27] for the reactants and expected products in the system studied are listed in Table 6.

3.3.1. Zn/lead oxides

The following reaction equations and stoichiometric mass percentages of Zn are based on the assumption that Zn reacts completely with the oxygen supplied by the lead oxides to form ZnO

Table 6
Thermodynamic data for reactants and products (298 K and 1 atm)

Compound	$\Delta_f H^\ominus$/ (kJ mol^{-1})	Molar mass/ (g mol^{-1})	Heat capacity/	
			(J K^{-1} g^{-1})	(J K^{-1} mol^{-1})
Zn	0	65.38	0.3849	25.17
ZnO	−348	81.38	0.4946	40.25
Pb	0	207.2	0.1590	32.94
PbO_2	−277	239.2	0.2557	61.16
$(Pb_3O_4)/3$	−245	685.6	0.2259	154.9
PbO	−218	223.2	0.2051	45.78
BaO_2	−648	169.3	0.3508	59.40
SrO_2	−651	119.6	0.4924	58.90
$KMnO_4$	−813	158.0	0.7544	119.2

Table 7
Calculated thermochemical data for the Zn/oxidant pyrotechnic reactions

System	Stoich. Zn/%	$\Delta_r H^\ominus$/ [kJ(mol Zn)$^{-1}$]	Q/(J g^{-1})	Heat cap./ (J K^{-1} g^{-1})	Combust. Temp./°C		Reacted
					Calc.	Meas.	
Zn/PbO_2	35.4	−210	1140	0.302	3800	>1800	
Zn/Pb_3O_4	27.6	−164	704	0.270	2630	>1800	
Zn/PbO	22.7	−130	450	0.246	18.50	>1800	
Zn/BaO_2	27.9	−270	1149	0.360	3220	1100 [a]	34
Zn/SrO_2	35.3	−299	1618	0.454	3590	1200 [a]	33
$Zn/KMnO_4$	29.3	−477	2138	0.134	3858	1700	44

[a] Temperature profiles of uncompacted mixtures.

$$2Zn + PbO_2 \rightarrow Pb + 2ZnO \quad (35.4\%\ Zn)$$

$$4Zn + Pb_3O_4 \rightarrow 3Pb + 4ZnO \quad (27.6\%\ Zn)$$

$$Zn + PbO \rightarrow Pb + ZnO \quad (22.7\%\ Zn)$$

The calculated standard enthalpies of reaction (per mole of Zn), the heat capacities, and the predicted adiabatic temperature rises ΔT, for the stoichiometric systems are shown in Table 7. These indicate that, if reaction were to approach completion, the temperatures reached during combustion of these pyrotechnic mixtures would be high.

3.3.2. *Zn/peroxides*

Similar thermochemical calculations for the Zn/peroxide systems, assuming the reactions

$$Zn + BaO_2 \rightarrow ZnO + BaO \quad (27.9\%\ Zn)$$

$$Zn + SrO_2 \rightarrow ZnO + SrO \quad (35.3\%\ Zn)$$

are given in Table 7. Predicted temperatures are compared with measured maximum temperatures and extents of reaction are estimated to be about 30–40%.

3.3.3. *Zn/potassium permanganate*

If ZnO is formed by reaction of Zn with the O_2 liberated during the decomposition of $KMnO_4$, the following reaction equations and stoichiometry apply for each decomposition step

$$12Zn + 10KMnO_4 \rightarrow 2.65K_2MnO_4 + (2.35K_2O,\ 7.35\ MnO_{2.05}) + 12ZnO \quad (33.2\%\ Zn)$$

$$6.8Zn + 10K_2MnO_4 \rightarrow 5.7K_3MnO_4 + 0.5\ (2.9K_2O,\ 8.5\ MnO_{2.1}) + 6.8ZnO \quad (18.4\%\ Zn)$$

This leads to an overall reaction equation

$$13.8Zn + 10\ KMnO_4 \rightarrow 1.51K_3MnO_4 + 0.133(2.9K_2O,\ 8.5MnO_{2.1}) + (2.35K_2O,\ 7.35MnO_{2.05}) + 13.8ZnO\ (36.3\%\ Zn)$$

Thermochemical calculations for the $Zn/KMnO_4$ system are shown in Table 7.

The above calculations have assumed that Zn forms ZnO in the reactions, but the reactions are probably more complex with possible formation of mixed zinc metal oxides. They may include $PbZnO_2$ and $PbZnO_3$ in the Zn/lead oxides systems, $BaZnO_2$ and $SrZnO_2$ in the Zn/peroxide systems, and $K_2Zn_6O_7$, K_2ZnO_2, and Mn_2ZnO_4 in the $Zn/KMnO_4$ system. Generally, appropriate thermodynamic data are not available.

3.4. Scanning electron microscopy (SEM)

A sample of Zn powder which had been oxidised in air had a crusty surface, with thin needles of ZnO being prominent [28]. The appearance of crystallites and the maintenance of approximately spherical assemblages supports the reports [2] of formation of solid ZnO on molten Zn surfaces.

The spongy appearance of the residues of combustion of the Zn/PbO_2 and Zn/Pb_3O_4 systems indicated gas evolution. In the Zn/PbO_2 system, compositions low in Zn (20–35% Zn) showed small, hexagonal crystallites and distinct plate formation. Melting and small spheres of product were apparent. Compositions higher in Zn (35% and up) showed not only molten regions, but also unreacted Zn. Globules of product were also visible. The Zn/Pb_3O_4 residues show similar features to the Zn/PbO_2 residues, most notably molten regions, partially reacted and unreacted Zn, and some plate formation.

The residue from the combustion of 50% Zn/BaO_2 (a considerable excess of zinc above the assumed stoichiometric ratio of 26% zinc) shows particles (of oxidant, product of oxidant decomposition, or reaction product) embedded in a matrix of solidified liquid. Most of the embedded particles have the size and shape of the original BaO_2 particles, but there were some spherical particles which could be isolated zinc droplets which have oxidised as spheres. Temperature profiles give a maximum temperature between 1000 and 1200°C. The temperature is higher than the melting point of zinc (420°C), but considerably lower than the melting points of the possible oxide products of ZnO (m.p. 1975°C) and BaO (m.p. 1918°C).

The residue from combustion of 30% Zn/SrO_2 (a slight stoichiometric deficit from the ratio of 36.3% Zn) showed melting of the zinc and some patches of the oxidant which had not been reached by the liquid. There was a spherical sub-structure to some of the melted regions which suggested either only surface melting and sintering of zinc particles during passage of the combustion front, or that isolated zinc droplets have reacted to form a ZnO layer before being engulfed by molten zinc. The residue of combustion of a richer zinc composition (50% Zn/SrO_2) showed fewer signs of extensive melting. Although residue particles were generally rounded, the surfaces were less smooth, suggesting some recrystallisation of products.

The residues of combustion of the $Zn/KMnO_4$ system contained holes indicating gas evolution. Surfaces were crumbly and showed roundish plates in some regions, and conglomerates of tiny granules in others. Molten regions and needle-like crystals were also visible.

4. Conclusions

DTA studies [1] showed that, in all of the zinc/oxidant systems considered, reactions take place above the melting point of zinc and are thus reactions of liquid zinc, either with solid oxidant, or with O_2 gas evolved during the decomposition of the oxidant.

Zn/PbO_2 compositions burned (2.2–90 mm s^{-1}) under compaction, evolving much gas. Zn/Pb_3O_4 compositions burnt erratically under minimal compaction, but the Zn/PbO system failed to sustain combustion when compacted. ZnO, PbO, and Pb were the major reaction products. Zn/BaO_2 and Zn/SrO_2 compositions did not burn under more than very light (450 kPa) compaction. The products of combustion were mixed oxides with little or no BaO or SrO.

Mixtures of $Zn/KMnO_4$ burned over the range 30–75% Zn under up to 150 MPa compaction. The burning rates ranged from 2 to 74 mm s^{-1}. The burning rates of mixtures containing less than 55% Zn were slow and reproducible, but reaction was more rapid and gaseous in more fuel-rich compositions. The rate of this fast reaction was decreased at higher compaction pressures, suggesting the possibility of two reactions mechanisms: a diffusion-type reaction in compositions low in Zn, and a more dominant reaction involving Zn vapour in fuel-rich compositions. Thermal analysis studies of this system [1] suggested that Zn diffuses into the solid residue formed during the first stage of the $KMnO_4$ decomposition. A reaction exotherm starting at 520°C was observed and is attributed to the reaction of Zn with this "K_2MnO_4" residue.

For those systems which burnt over a range of compositions (Zn/PbO_2 and $Zn/KMnO_4$), there was a marked and very similar increase in burning rate with increasing proportion of zinc. Evidence from thermal analysis [1] and SEM shows that the initial reaction involves molten zinc. Visual observation of burning and some of the micrographs of combustion residues indicate significant production of gas and, since this increases with the proportion of zinc, formation of zinc vapour must occur. The participation of both liquid and gaseous fuel in reaction with solid oxidants, or oxygen gas produced by decomposition of the oxidants, would give rise to a variety of reaction paths and could explain the extreme sensitivity of zinc/oxidant systems to compaction. The surface tension of zinc at its melting point [27] is high (relative to other low melting point metals, e.g. about twice that of Sb and Pb) and hence movement of liquid zinc through pores and channels will not occur all that readily, and oxidant surfaces will not be easily wetted.

Temperature profiles generally showed steps, suggesting that more than one reaction occurs.

Comparison of the behaviour of the $Zn/KMnO_4$ system with that of the widely-used $Sb/KMnO_4$ system [20,21,29] is of interest because Sb melts at a much higher temperature (631°C) than Zn (420°C). Thermal analyses [29] showed that oxidation of solid Sb in air occurs in several stages with initial onset at about 230°C, and that the oxides formed are volatile above about 450°C. Zn, on the other hand, is oxidised mainly as the liquid and the ZnO formed is not volatile. Behaviour on combustion would thus be expected to be considerably different. The range of burning rates of the $Sb/KMnO_4$ system (combustion temperatures about 1500°C) over a wide range of compositions, fuel particle-sizes and proportions of Sb_2O_3 as additive, was more limited at the higher end (2–15 mm s^{-1}) than for the $Zn/KMnO_4$ system (combustion temperature 1700°C or higher). (The lower limit of burning rates is associated with heat-loss factors for the channel used.) The $Se/KMnO_4$ system [21] burnt over only a limited range of compositions (22–30% Se) at about 2.5 mm s^{-1} and with a relatively low combustion temperature of about 1000°C. Se melts at 220°C. It thus appears as if the combustion temperature is an important factor in determining the burning rate.

ZnO is an excess metal oxide and BaO_2 and SrO_2 are very much metal-deficit compounds relative to BaO and SrO. Assuming that the initial stages of reaction involve some formation of ZnO which is then in contact with MO_{1+x}, where M is Ba or Sr, the tendency will be for excess Zn in the ZnO (as Zn^{2+} interstitials?) to move into the MO_{1+x} lattice (via M^{2+} vacancies?). Because the ionic radii are $Zn^{2+} = 0.075$ nm, (metal 0.137 nm), $Ba^{2+} = 0.136$ nm and $Sr^{2+} = 0.113$ nm, it can be argued that reaction within the more spacious BaO_2 lattice should be favoured. This is the trend shown by the E_a values. SrO_2 does however decompose at lower temperatures and with a lower ΔH value than BaO_2. This could be compensated for by a catalytic effect on the peroxide decomposition of the Zn^{2+} which has penetrated the BaO_2 lattice.

Drennan and Brown [30] have reported on studies of the combustion of the Mn/BaO_2, Mo/BaO_2, Mn/SrO_2 and Mo/SrO_2 systems, and Tribelhorn et al. [31] on the Fe/BaO_2 and Fe/SrO_2 systems. The relevant radii are: Mn metal, 0.137 nm; Mo metal, 0.140 nm; Mn^{2+}, 0.067 nm; Mn^{3+}, 0.058 nm; Mn^{7+}, 0.026 nm; Mo^{3+}, 0.067 nm; Mo^{4+}, 0.065 nm; Mo^{6+}, 0.060 nm; Fe metal, 0.124 nm; Fe^{2+}, 0.074 nm; Fe^{3+}, 0.064 nm; Ba^{2+}, 0.136 nm; and Sr^{2+}, 0.113 nm. Diffusion via cation vacancies in the oxidant structure should thus be favoured in the BaO_2 lattice relative to the SrO_2 lattice, but, for comparable oxidation states, differences between the behaviour of Mn and Mo, based on geometry, should be slight. Based on the same mass percentage of fuel, or on the same mole ratio, the binary fuel/peroxide systems had burning-rates in the order [32] $Mn/SrO_2 > Mn/BaO_2 > Mo/BaO_2 > Mo/SrO_2$.

Inclusion of the Fe- and Zn-fuelled systems, which all had greater rates of burning than the Mn- and Mo-fuelled systems, gave the following series of maximum rates of burning: $Zn/BaO_2 > Fe/BaO_2 > Zn/SrO_2 > Fe/SrO_2 > Mn/SrO_2$.

Activation energies derived from combustion studies were in the order $Fe/BaO_2 < Zn/SrO_2 < Mn/BaO_2 < Zn/BaO_2 < Mn/SrO_2 \approx Mo/BaO_2 < Mo/SrO_2 < Fe/SrO_2$, so these results do not follow the predictions based on cation diffusion.

In a trend opposite to the Si/oxidant systems studied by Rugunanan and Brown [33], lower activation energies are associated with slower burning rates in the Mo- and Mn-fuelled systems. Although Mn and Mo appear at the extremes of the above set of Mn/peroxide and Mo/peroxide systems, the suggestion that the properties of the fuels are more important than the properties of the oxidants does not apply generally, as the effect of the peroxide can clearly be seen in studies on the Fe- and Zn-fuelled systems. The melting point of Mn (1244°C) is far lower than that of Mo (2610°C), so that Mn is likely to be molten at the combustion temperatures (1350 > 1800°C). Similarly, Fe melts at 1535°C, approximately the maximum temperature attained in the Fe/peroxide systems, but Zn melts at 419°C, well below the reaction temperature of Zn/peroxide systems. Examination of the products of combustion showed that oxidation of the metals was generally incomplete, probably because of the formation of protective layers of oxide. Both the temperature and the energy requirements for dissociation are lower for SrO_2 than for BaO_2, so the trends above could be explained on the basis of some preliminary dissociation of the peroxides, followed by metal + O_2(g) → metal oxide. Oxidation of Mn powder, heated in O_2(g), began at lower temperatures than for Mo powder under the same conditions, but oxidation of Mo was complicated by sublimation of the product. Fe powder was found to oxidise at temperatures roughly 100°C lower than those of zinc, since the oxidation of zinc was only noticeable above the melting point of 419°C, under controlled heating conditions.

From the above discussion, it may be concluded that fuel/oxidant interactions may fit into one of several patterns lying between the extremes of solid–solid reactions involving diffusion of species derived from the fuel into the structure of the oxidant, oxidation of the fuel by gaseous products of oxidant decomposition, or even liquid–solid or liquid–vapour reactions. Detailed knowledge is needed of the thermal behaviour of the fuel in oxygen and of the structure and thermal characteristics of possible oxidation products, as well as of the thermal stability of the oxidant and any likely decomposition products. The participation of liquid and/or gaseous phases may be difficult to detect, but is of great practical importance.

SEM results show the heterogeneous nature of both the combustion process and the combustion products. Passage of the burning front through the fuel/oxidant mixture, which may contain clusters of fuel and/or oxidant particles may be too rapid for complete reaction to occur throughout. Measurements on the zinc/peroxide systems suggest extents of reaction of only 30–40%. This emphasises the importance of mixing to give reproducible burning, and the difficulties of the analysing combustion residues, and also highlights the associated problem of trying to obtain a uniform product by self-propagating high-temperature synthesis (SHS) [34].

A general conclusion is that, in spite of the environmental advantages of using zinc as a fuel, the systems studied here are not suitable for use as pyrotechnic delays. Because the unsuitability is not derived from properties of the oxidants, any zinc-fuelled system is likely to display similar erratic and gassy combustion.

Acknowledgements

The authors are indebted to Dr R.A. Rugunanan for his interest and comments, and to AECI Explosives Ltd. for financial support.

References

[1] M.J. Tribelhorn, D.S. Venables and M.E. Brown, Thermochim. Acta, in press.
[2] M.E. Derevyaga, L.N. Stesik and E.A. Fedorin, Fiz. Goreniya Vrzryva, 13 (1977) 852.
[3] J.O. Cope, Trans. Faraday Soc., 57 (1961) 493.
[4] P.G. Laye and E.L. Charsley, Thermochim. Acta, 120 (1987) 325.
[5] J.A.C. Goodfield and G.J. Rees, Fuel, 61 (1982) 843.
[6] S.R. Yoganarasimhan, N.S. Bankar, S.B. Kulkarni and R.G. Sarawadekar, J. Therm. Anal., 21 (1981) 283.
[7] R.L. Drennan and M.E. Brown, Thermochim. Acta, 208 (1992) 201, 223, 247.
[8] J.E. Spice and L.A.K. Staveley, J. Soc. Chem. Ind., 68 (1949) 313.
[9] J.E. Spice and L.A.K. Staveley, J. Soc. Chem. Ind., 68 (1949) 348.
[10] R.A.W. Hill, L.E. Sutton, R.B. Temple and A. White, Research, 3 (1950) 877.
[11] F. Booth, Trans. Faraday Soc., 49 (1953) 272.
[12] V.D. Hogan and S. Gordon, J. Phys. Chem., 61 (1957) 1401.
[13] S. Nakahara, J. Ind. Expl. Soc. Jpn., 22 (1961) 259.
[14] S. Nakahara and T. Hikita, J. Ind. Expl. Soc. Jpn., 21 (1960) 2.
[15] S. Nakahara and T. Hikita, J. Ind. Expl. Soc. Jpn., 20 (1959) 356.
[16] L.B. Johnson, Ind. Eng. Chem., 52 (1960) 241.
[17] R.A.W. Hill and A.A. Wallace, Nature, 178 (1956) 692.
[18] R.A.W. Hill, Trans. Faraday Soc., 53 (1957) 1136.
[19] D. Beyens and E. Dubois, 10th Int. Pyrotech. Sem., (1985) 17 1.
[20] M.W. Beck and M.E. Brown, 10th Int. Pyrotech. Sem., Fraunhofer Inst. für Treib- und Explosivstoffe, 1985, paper 14.
[21] M.W. Beck and M.E. Brown, Combust. Flame, 65 (1986) 67, 263.
[22] A. Savitzky and M.J.E. Golay, Anal. Chem., 36 (1964) 1627.
[23] T. Boddington, P.G. Laye, J.R.G. Pude and J. Tipping, Combust. Flame, 47 (1982) 235.
[24] T. Boddington, P.G. Laye, J. Tipping and D. Whalley, Combust. Flame, 63 (1986) 359.
[25] W.J. Dixon, BMDP Statistical Software Manual, University of California Press, 1988.
[26] R.A. Nyquist and R.O. Kagel, Infrared Spectra of Inorganic Compounds, Academic Press, New York, 1971.
[27] R.C. Weast, Handbook of Chemistry and Physics, CRC Press, Boca Raton, FL, 67th edn., 1986.
[28] C.D.S. Tuck, M.E. Whitehead and R.E. Smallman, Corr. Sci., 21 (1981) 333.
[29] M.W. Beck and M.E. Brown, Thermochim. Acta, 65 (1983) 197.
[30] R.L. Drennan and M.E. Brown, Thermochim. Acta, 208 (1992) 201, 223, 247.
[31] M.J. Tribelhorn, M.G. Blenkinsop and M.E. Brown, to be published.
[32] M.E. Brown, M.W. Beck, R.L. Drennan, R.A. Rugunanan, M.J. Tribelhorn and M.G. Blenkinsop, Proc. 4th Int. Symp. Expl. Technol. and Ballistics, Pretoria, (1992) 391.
[33] R.A. Rugunanan and M.E. Brown, Combust. Sci. Technol., 95 (1994) 61, 85, 101, 117.
[34] Z.A. Munir and J.B. Holt (Eds.), Combustion and Plasma Synthesis of high-Temperature Materials, VCH Publishers, New York, 1990.